

The C/O ratio at low metallicity: constraints on early chemical evolution from observations of Galactic halo stars [★]

D. Fabbian^{1,2}, P. E. Nissen³, M. Asplund⁴, M. Pettini⁵, C. Akerman⁵

¹ Research School of Astronomy & Astrophysics, The Australian National University, Mount Stromlo Observatory, Cotter Road, Weston ACT 2611, Australia

² Current address: Instituto de Astrofísica de Canarias, Calle Via Láctea s/n, E38205, La Laguna, Tenerife, España

³ Department of Physics and Astronomy, University of Aarhus, 8000 Aarhus C, Denmark

⁴ Max Planck Institute for Astrophysics, Postfach 1317, 85741 Garching b. München, Germany

⁵ Institute of Astronomy, University of Cambridge, Madingley Road, Cambridge CB3 0HA, UK

Received / Accepted

ABSTRACT

Aims. We present new measurements of the abundances of carbon and oxygen derived from high-excitation C I and O I absorption lines in metal-poor halo stars, with the aim of clarifying the main sources of these two elements in the early stages of the chemical enrichment of the Galaxy.

Methods. We target 15 new stars compared to our previous study, with an emphasis on additional C/O determinations in the crucial metallicity range $-3 \lesssim [\text{Fe}/\text{H}] \lesssim -2$. The stellar effective temperatures were estimated from the profile of the H β line. Departures from local thermodynamic equilibrium were accounted for in the line formation for both carbon and oxygen. The non-LTE effects are very strong at the lowest metallicities but, contrary to what has sometimes been assumed in the past due to a simplified assessment, of different degrees for the two elements. In addition, for the 28 stars with $[\text{Fe}/\text{H}] < -1$ previously analysed, stellar parameters were re-derived and non-LTE corrections applied in the same fashion as for the rest of our sample, giving consistent abundances for 43 halo stars in total.

Results. The new observations and non-LTE calculations strengthen previous suggestions of an upturn in C/O towards lower metallicity (particularly for $[\text{O}/\text{H}] \lesssim -2$). The C/O values derived for these very metal-poor stars are, however, sensitive to excitation via the still poorly quantified inelastic H collisions. While these do not significantly affect the non-LTE results for C I, they greatly modify the O I outcome. Adopting the H collisional cross-sections estimated from the classical Drawin formula leads to $[\text{C}/\text{O}] \approx 0$ at $[\text{O}/\text{H}] \approx -3$. To remove the upturn in C/O, near-LTE formation for O I lines would be required, which could only happen if the H collisional efficiency with the Drawin recipe is underestimated by factors of up to several tens of times, which we consider unlikely.

Conclusions. The high C/O values derived at the lowest metallicities may be revealing the fingerprints of Population III stars or may signal rotationally-aided nucleosynthesis in more normal Population II stars.

Key words. Stars: abundances, late-type – Galaxy: abundances, evolution

1. Introduction

Carbon and oxygen play a fundamental role in the chemical evolution of the Universe. They rank as the most common elements produced via stellar life and death, and their abundances are surpassed only by those of H and He, which are instead linked to the Big Bang.

The abundances of carbon and oxygen may be important in relation to a transition from massive Population III stars to a low-mass Population II star formation mode. The latter encompasses the birth mechanism of the oldest stellar population currently known, including the most iron-deficient stars in the halo, which are thought to carry the fingerprints of at most a few supernovae. The very first

stars in the Universe are predicted to have been very massive, because the absence of metals (and thus, of cooling by fine-structure lines of C and O) only allowed fragmentation on large scales. The first lower-mass ($\lesssim 1M_{\odot}$) stars would then only have formed once a critical metallicity (allowing cloud fragmentation into smaller clumps) was reached in the early Universe thanks to enrichment of elements ejected from the first supernovae. Bromm & Loeb (2003) suggest that no low-mass dwarf star should exist having (*simultaneously*) $[\text{C}/\text{H}] \lesssim -3.5$ and $[\text{O}/\text{H}] \lesssim -3$. They also point out that, in order to sample individual supernova events occurring in the earliest epochs, the best candidates among these second generation stars would be those with abundances of carbon and oxygen very close to this critical metallicity. Frebel, Johnson & Bromm (2007) predict that all stars with $[\text{Fe}/\text{H}] < -4$ should show enhanced C and/or O abundances, because otherwise they would not have lived long enough (have low enough mass) to be observed.

In this context, it is interesting to note that, very recently, Carollo et al. (2007) have highlighted that our

Send offprint requests to: D. Fabbian,
e-mail: damian@mso.anu.edu.au

[★] Based on data collected with the European Southern Observatory's *Very Large Telescope* (VLT) at the Paranal, Chile (programmes No. 67.D-0106 and 73.D-0024) and with the *Magellan Telescope* at Las Campanas Observatory, Chile

Galaxy has a second, more distant halo structure (the “outer halo”) with a lower peak metallicity and probably different (dissipationless) formation mechanism than the inner halo.

Despite our knowledge of the nuclear processes involved (see e.g. reviews by Wallerstein et al. 1997 and El Eid 2005), the constraints on the actual sources of carbon in the Galaxy are still not satisfying. There is ongoing debate on whether the bulk of carbon yields is mainly contributed by massive stars (e.g. Carigi et al. 2005) or low- and intermediate-mass stars (e.g. Chiappini, Romano & Matteucci 2003).

In a number of investigations (e.g. Andersson & Edvardsson 1994; Gustafsson et al. 1999; Reddy, Lambert & Allende Prieto 2006), the [C/Fe] abundance ratio in the thin disc has been found to slowly decrease with time and increasing metallicity. The work of Bensby & Feltzing (2006) suggests that [C/Fe] flattens to roughly the solar value at intermediately-low metallicities ($-1 < [\text{Fe}/\text{H}] < 0$). This trend is robust to non-LTE effects (Fabbian et al. 2006), since that study employs the forbidden [C I] line at 8727 Å. However, when moving to the halo stellar population, this absorption feature becomes too weak. Akerman et al. (2004) have investigated the derivation of accurate abundances from high-excitation infrared C I lines, detected down to $[\text{Fe}/\text{H}] \sim -3.2$. Fabbian et al. (2006) have pointed out how at these low metallicities, after accounting for non-LTE effects, a roughly flat plateau is evident at a level of $[\text{C}/\text{Fe}] \approx 0$, even though a relatively large (and possibly real) scatter remains.

Oxygen is thought to be synthesized in short-lived massive stars, which end their lives as type II SNe, dispersing their chemical make-up into the interstellar medium (ISM). Despite many studies, the chemical evolution of oxygen during the early history of the Milky Way is still debated and not well understood, giving rise to the so-called “oxygen problem”. Different abundance indicators give conflicting results for halo stars, either a linear increase with decreasing metallicity, reaching $[\text{O}/\text{Fe}] \approx +1.0$ dex at $[\text{Fe}/\text{H}] = -3$, when using UV OH lines (Israelian et al. 1998; Boesgaard et al. 1999) or a flat plateau when using the forbidden [O I] 6300 Å line (Barbuy 1988; Nissen et al. 2002; García Pérez et al. 2006), while the O I 7772 – 7775 Å triplet in metal-poor unevolved stars typically implies values between those two extreme trends. This problem is crucial, since the adopted oxygen abundance influences, for example, the derived ages of globular clusters and the production of Li, Be, and B from spallation of C, N, and O atoms in the early Galaxy.

For oxygen there are several potential pitfalls in the analysis that can result in systematic errors. The unresolved issue of the correct effective temperature (T_{eff}) scale at low metallicities is clearly important, since it affects OH and O I in opposite ways (Meléndez et al. 2006). For molecules like OH, the very different atmospheric temperature structure in 3D hydrodynamical model atmospheres compared with standard 1D hydrostatic models leads to very large negative 3D abundance corrections (Asplund & García Pérez 2001; Collet, Asplund & Trampedach 2007). The [O I] line is also sensitive to such 3D effects but not as severely (Nissen et al. 2002). While it has been known for a long time that the O I 7772 – 7775 Å lines are prone to departures from LTE (e.g. Kiselman 1991; Asplund et al. 2004), Fabbian

et al. (2008a) have very recently demonstrated how the relevant non-LTE corrections are likely to have been underestimated due to inadequate collisional data being used in the construction of the atomic models employed. The outcome of using an up-to-date such model, including accurate electron collisional cross-sections obtained through quantum mechanical calculations, is a sharp increase in the non-LTE effects for $[\text{Fe}/\text{H}] \lesssim -2.5$. The physical explanation is in terms of radiative pumping in the UV resonance lines and efficient intersystem collisional coupling.

Early observational results (Tomkin et al. 1992) showed that [C/O] is subsolar when $[\text{O}/\text{H}] < 0$, and suggested that the ratio remains essentially flat at this level down to low metallicities. More recently, renewed attention has been given to investigating the behaviour of the [C/O] ratio with decreasing metallicity. By looking respectively at metal-poor dwarf stars and giant stars in the halo of our Galaxy, Akerman et al. (2004) and Spite et al. (2005) suggested that [C/O] increases again at very low metallicities, recovering near-solar values when $[\text{O}/\text{H}] \simeq -3$. Unfortunately, different abundance indicators were used in the two investigations, so that the results of these two studies may not be directly comparable. However, the suggestion of high [C/O] values at the lowest metallicities is potentially very important and deserving of further scrutiny, as it may be an indication of C-rich ejecta from massive Population III SNe.

As reliable non-LTE corrections to the C and O abundances in late-type stars were not available at the time, Akerman et al. (2004) assumed that the C I lines near 9100 Å would be subject to the same non-LTE effects as the IR oxygen triplet lines, given that all these spectral features arise from highly excited levels. However, recent analyses of the problem (Fabbian et al. 2006, 2008a) have shown that the abundance corrections for both elements are likely to be more negative than previously assumed. In particular, for typical low-metallicity halo stars such corrections amount to ~ -0.4 dex for carbon and ~ -0.9 for oxygen, ignoring the still very uncertain effects of inelastic H collision. Including the collisions in accordance with the classical Drawin (1968, 1969) recipe, reduces the magnitude of the corrections which, however, remain significant (in particular, ~ -0.5 dex for O).

Complementary information on the nucleosynthetic origin of C and O at low metallicity is also available from high-redshift observations of metal-poor damped Lyman-alpha systems (DLAs) which are generally interpreted as galaxies in early stages of chemical evolution (Wolfe, Gawiser, & Prochaska 2005). For example, Erni et al. (2006) found the chemical abundances in a DLA with $[\text{O}/\text{H}] \sim -2.5$ to be consistent with enrichment from a single starburst of massive ($10 - 50 M_{\odot}$) zero-metallicity stars. Pettini et al. (2008) very recently derived near-solar [C/O] ratios in a small sample of the most metal-poor DLAs/subDLAs known.

Becker et al. (2006) studied absorption toward high-redshift ($4.9 < z < 6.4$) quasars, inferring a mean $[\text{C}/\text{O}] \sim -0.3$ in the Lyman alpha forest clouds which trace the low-density and low-metallicity intergalactic medium (IGM). At lower redshifts, ($2.1 < z < 3.6$), Aguirre et al. (2008) deduced $[\text{C}/\text{O}] = -0.66 \pm 0.2$. While broadly in line with halo star abundances, these IGM values are difficult to interpret because: (a) they rely on the accuracy of large photoionisation corrections, and (b) the origin of the metals found in

the IGM is still unclear (e.g. Ryan-Weber et al. 2006 and references therein).

In the present study, we aim to use halo stellar abundances as tracers of early Galactic chemical evolution, by deriving carbon and oxygen compositions in non-LTE for a new set of metal-poor stars, as well as carrying out an improved analysis of previous data. The results provide an important test for Galactic chemical evolution models.

2. Observations and data reduction

The stellar sample employed in this study is mainly composed of observations carried out at the European Southern Observatory’s Very Large Telescope (ESO VLT) using its two-arm, cross-dispersed, high-resolution Ultraviolet-Visual Echelle Spectrograph (UVES, see Dekker et al. 2000) mounted on the UT2 (Kueyen telescope).

The dataset is composed of spectra for 12 very metal-poor stars observed in 2004, together with spectra of 28 halo stars with $[\text{Fe}/\text{H}] < -1$ (from Akerman et al. 2004) for which we re-derived stellar parameters in a consistent fashion with the new stars. This UVES sample is the same as that used by Nissen et al. (2007); therefore we direct the reader to the description of the observations therein. Here we just mention that the UVES spectra cover the blue region 3800 – 5000 Å and the near-IR region 6700 – 10500 Å, both with a resolving power $R \equiv \lambda/\Delta\lambda \simeq 60\,000$. The blue region contains Fe I and Fe II lines from which we determine $[\text{Fe}/\text{H}]$, and the $\text{H}\beta$ line used for deriving the effective temperature of the stars. The C I and O I lines are found in the near-IR region.

Spectra of four additional stars were obtained with the Magellan 6.5 m telescope over three nights in December 2003. The Magellan Inamori Kyocera Echelle (MIKE), a high-throughput double echelle spectrograph (Bernstein et al. 2003), was used. The entrance slit was set at 0.35 arcsec, which corresponds to a resolving power $R \simeq 60\,000$, i.e. the same as the UVES spectra, but with only two pixels per spectral resolution element compared to four pixels for the near-IR UVES spectra. The MIKE spectra cover, however, broader spectral ranges than UVES, i.e. 3300 – 4900 Å in the blue arm and 4900 – 10000 Å in the red arm. Actually, the blue part was not used, mainly because the $\text{H}\beta$ line is not sufficiently well centered in an echelle order to derive T_{eff} with the technique applied by Nissen et al. (2007). Instead, T_{eff} was derived from $\text{H}\alpha$ as described by Asplund et al. (2006), and $[\text{Fe}/\text{H}]$ was determined from Fe II lines in the 4900 – 6700 Å region.

Since one of the stars in the MIKE sample, G48-29, was also observed in our UVES 2004 run, this brings the total of newly observed targets to 15. Together with the observations by Akerman et al. (2004), a total of 43 halo stars are thus employed in the present study.

The new spectra were reduced with the standard echelle data reduction package in IRAF. Background subtraction, flat-fielding, order extraction and wavelength calibration were done using semi-automatic IRAF routines. The C I lines are located in a part of the optical spectrum affected by the presence of strong telluric water vapour lines. Thus, spectra were obtained and processed not only for the programme stars but also for hot, fast-rotating, B-type stars,

Table 1. The IDs and atmospheric parameters (effective temperature, gravity and iron content) of the halo stars observed. Our sample includes 28 stars from the 2001 UVES run and having $[\text{Fe}/\text{H}] < -1$. For such objects T_{eff} was re-determined by us consistently with the rest of the sample.

ID	T_{eff}	$\log g$	$[\text{Fe}/\text{H}]$
UVES (2001)			
BD-13° 3442	6366	3.99	-2.69
CD-30° 18140	6272	4.12	-1.89
CD-35° 14849	6294	4.26	-2.34
CD-42° 14278	6085	4.39	-2.03
G011-044	6178	4.35	-2.03
G013-009	6343	4.01	-2.29
G018-039	6093	4.19	-1.46
G020-008	6194	4.29	-2.19
G024-003	6084	4.23	-1.62
G029-023	6194	4.04	-1.69
G053-041	5993	4.22	-1.29
G064-012	6435	4.26	-3.24
G064-037	6432	4.24	-3.08
G066-030*	6470	4.29	-1.48
G126-062*	6224	4.11	-1.55
G186-026	6417	4.42	-2.54
HD106038	6027	4.36	-1.37
HD108177	6156	4.28	-1.71
HD110621	6157	4.08	-1.59
HD140283	5849	3.72	-2.38
HD160617	6047	3.84	-1.75
HD179626	5881	4.02	-1.12
HD181743	6044	4.39	-1.87
HD188031	6234	4.16	-1.72
HD193901	5699	4.42	-1.10
HD194598	6020	4.30	-1.15
HD215801	6071	3.83	-2.28
LP815-43	6483	4.21	-2.71
UVES (2004)			
CD-24 17504	6338	4.32	-3.21
CD-71 1234*	6325	4.18	-2.38
CS 22943-0095	6349	4.18	-2.24
G004-037	6308	4.25	-2.45
G048-029**	6482	4.25	-2.60
G059-027*	6272	4.23	-1.93
G126-052	6396	4.20	-2.21
G166-054	6407	4.28	-2.58
HD84937	6357	4.07	-2.11
HD338529	6373	4.03	-2.26
LP635-014	6367	4.11	-2.39
LP651-004	6371	4.20	-2.63
MIKE (2003)			
G041-041	6440	4.06	-2.66
G048-029**	6489	4.25	-2.61
G084-029	6302	4.05	-2.62
LP831-70	6232	4.36	-2.93

*Single-lined spectroscopic binary stars.

**This star was observed in both the UVES (2004) and MIKE (2003) runs.

which are necessary to effectively correct for such atmospheric disturbance in the infrared. The IRAF task “telluric” was used to divide the spectrum of our sample stars by those of the comparison B-type stars. We then used the task “continuum” to normalize the spectra (continuum

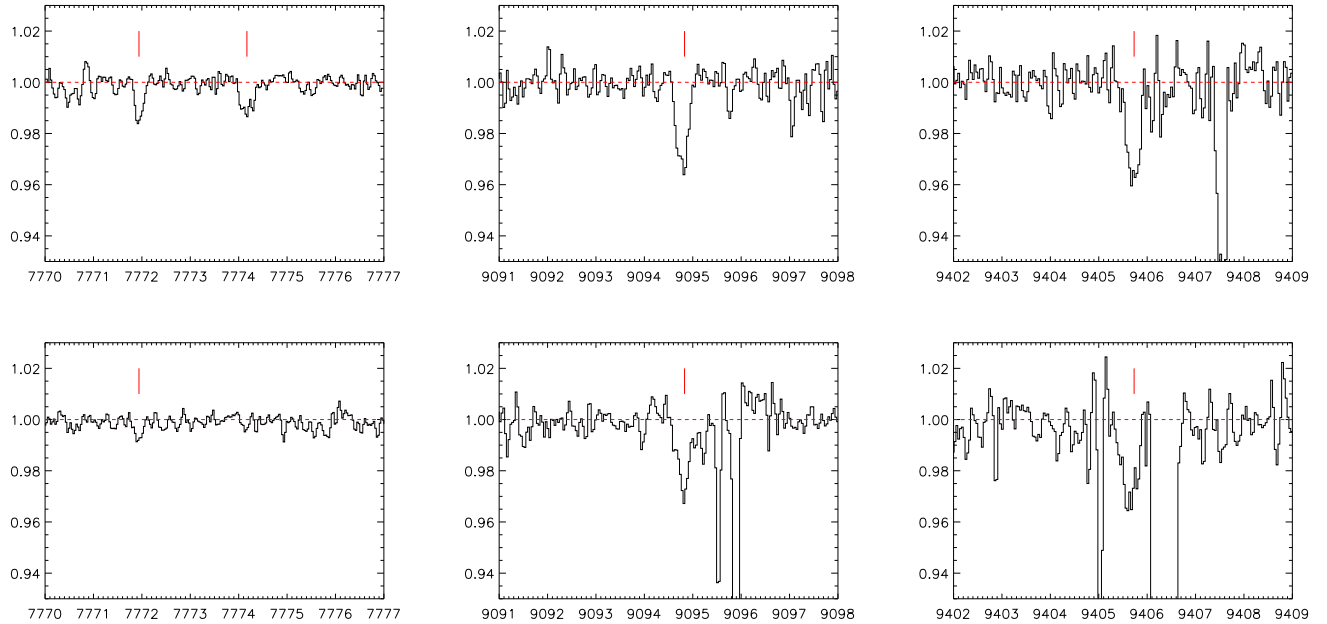


Fig. 1. The spectral quality in the regions near the O I (left panels) and C I (middle and right panels) high-excitation lines is shown for two of the most metal-poor stars (G64-37, at $[\text{Fe}/\text{H}] = -3.08$, upper panels, and CD-24 17504, at $[\text{Fe}/\text{H}] = -3.21$, lower panels) in the sample, with wavelength (in \AA) on the horizontal axis and flux (normalized to the continuum level) on the vertical one. The spectra have $\text{S/N} \sim 200$ and ~ 400 , respectively, in the O I triplet region. The S/N around the C I lines is a factor ~ 2 lower, and strong residuals from the removal of telluric lines are present. Spectral features of interest near 7774, 9095, and 9406 \AA for which we could determine reliable equivalent width estimates in these two stars are marked by short vertical ticks above the observed spectra.

placement). We corrected for the radial velocity Doppler shift by measuring the wavelengths of a few selected lines. Finally, equivalent widths were measured on the reduced spectra for the lines of interest by performing a Gaussian fit, or by direct integration in the case of very weak lines or poor fit due to noisy spectral regions.

The reduction of the MIKE spectra was complicated by the fact that the image of the slit is significantly tilted and curved on the CCD. Nevertheless, once this was accounted for, the final quality of the data proved to be similar to that of the UVES spectra. For stars with repeated observations on different nights we co-added the individual spectra to improve the final signal-to-noise ratio. Overall, the new data are of similar, or higher, quality than those in the study by Akerman et al. (2004). The typical signal-to-noise ratios per pixel around the C I and O I spectral features of interest are $\text{S/N} = 200 - 400$, the region encompassing the oxygen triplet having higher S/N than that around the high-excitation carbon lines (see Fig. 1).

Generally, all spectral lines of interest in this study were detectable in the UVES spectra thanks to the relatively high S/N obtained. Even in the case of CD-24 17504, the most metal-poor ($[\text{Fe}/\text{H}] = -3.21$) star among the 15 newly observed, we were able to derive reliable estimates of the carbon and oxygen abundances from the strongest lines in the multiplets targeted. For oxygen in particular, the equivalent width measured is only 1.7 m\AA , but the reliability of the derived abundance was confirmed via spectral synthesis (see Subsection 3.2). Regarding the Magellan observations, it was possible to achieve on average similarly high S/N . This is somehow offset by lower pixel sampling than in the

UVES spectra and by rapid drop in the MIKE CCD sensitivity beyond 9200 \AA , the latter implying that the S/N is too low for a detection at low metallicity of C I 9405.7 \AA (which also falls very close to the edge of an echelle order) in the midst of strong telluric lines. This therefore makes C I 9094.8 \AA and 9111.8 \AA the only useful lines for deriving the carbon abundance in this case. These C I lines are however not clearly detectable in LP831-70, the most metal-poor object in the sample observed with MIKE, even though the star was observed on all three nights and all spectra were combined to achieve a high $\text{S/N} \sim 380$ per pixel. In particular, due to an overlapping water vapour feature, even the stronger 9094.8 \AA line is not measurable. We estimated upper limits to the carbon and oxygen abundances in this star by measuring the equivalent widths (typically a few m\AA) of noise features.

3. Elemental abundance analysis

3.1. Stellar parameters

Estimates of the effective temperatures for all stars in this study, including those with $[\text{Fe}/\text{H}] < -1$ in the Akerman et al. (2004) sample, were derived using the $\text{H}\beta$ line profile. For a detailed discussion of the procedure and the improved accuracy of the T_{eff} determinations, see Nissen et al. (2007). As discussed therein, differential values are determined with a *precision* of $\sim 30 \text{ K}$ for metal-poor turnoff stars. Below, we compare with effective temperature estimates from other methods.

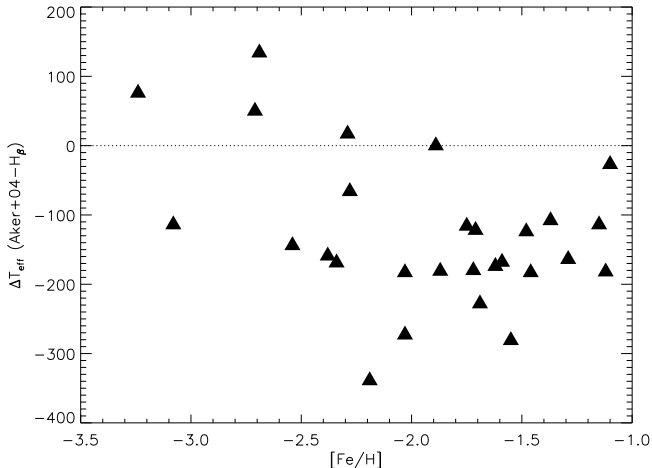


Fig. 2. Run of ΔT_{eff} (the difference between effective temperature determinations in Akerman et al. 2004 and in this work) against metallicity.

Akerman et al. (2004) derived their T_{eff} values from $(b-y)$ and $(V-K)$ colour indices. Fig. 2 shows the difference between their and our T_{eff} values for the stars with $[\text{Fe}/\text{H}] < -1$ in common between the two studies. For the six metal-rich stars with $[\text{Fe}/\text{H}] > -1$ in the Akerman et al. sample, it is very hard to determine accurate temperatures from $\text{H}\beta$ because of many blending metal lines across its profile. Those stars are not included in the present investigation, since we are mainly interested in the behaviour of C/O at very low $[\text{Fe}/\text{H}]$. Inspection of Fig. 2 shows that our temperature estimates are typically 150 K higher than those by Akerman et al. (2004) down to $[\text{Fe}/\text{H}] \sim -2.6$, with a few stars showing a difference of up to ~ 300 K, while a few others have very similar determinations in the two studies. In contrast, our estimated effective temperatures tend to be lower (for three out of four stars) at very low metallicities.

The advantage of the $\text{H}\beta$ method is that errors in gravity, metallicity and in interstellar reddening do not affect the determination of T_{eff} . A comparison with T_{eff} values based on $V-K$ calibrations (Alonso et al. 1996; Ramírez & Meléndez 2005b; Masana, Jordi & Ribas 2006) shows that the difference with those estimates tends to switch sign (and become larger) with decreasing metallicity. The $\text{H}\beta$ -based temperatures are higher by 50–100 K when $[\text{Fe}/\text{H}] > -2$, but lower by about 100 K for $[\text{Fe}/\text{H}] < -2.5$. In the transition region, $-2.5 \leq [\text{Fe}/\text{H}] \leq -2$, there is a large scatter (Nissen et al. 2007). This is essentially the same behaviour as just discussed when comparing with the estimates by Akerman et al. (2004), except that in that case the residuals are larger in the $[\text{Fe}/\text{H}] > -2$ regime. This is due to a systematic offset of ~ 50 –100 K in the values of T_{eff} derived by Akerman et al. (2004) compared with those by Ramírez & Meléndez (2005b) and Masana et al. (2006).

Masana and co-workers suggested that temperature estimates from the infrared flux method (IRFM) may be too high by ~ 200 K for $[\text{Fe}/\text{H}] < -2.5$. However, the $V-K$ calibrations by Masana et al. are in fairly good agreement with the Ramírez & Meléndez scale for our sample of stars. On the other hand, in their calibrations, Masana et al. give

two equations: one valid for $0.35 < (V-K)_0 < 1.15$ and the other for $1.15 \leq (V-K)_0 < 3.0$. One would then expect a continuous transition between T_{eff} estimates obtained with the two calibrations. However, this is not the case. Since many metal-poor turnoff stars have indeed $(V-K)_0$ values close to 1.15, the final result will depend on whether a star, after reddening correction, happens to fall below or above that value, with important differences in the T_{eff} derived in the two cases, amounting to ~ 200 K at very low $[\text{Fe}/\text{H}]$. In particular, most of the largest discrepancies (> 100 K) occur for values around the mentioned discontinuity, within ± 0.1 of $(V-K)_0 = 1.15$. It therefore appears that the Masana et al. calibrations may systematically overestimate T_{eff} around $(V-K) \approx 1.15$.

In any case, this apparent inconsistency can not straightforwardly explain the differences with the $\text{H}\beta$ -derived temperatures, since the resulting T_{eff} values from the equations by Masana et al. agree reasonably well with those from the Ramírez & Meléndez calibrations, which apparently have no such inconsistencies. Our $\text{H}\beta$ -derived temperatures may thus be too low by ~ 100 K at the lowest metallicities. In general, $(V-K)$ calibrations are bound to be less effective at very low metallicities, because of the small numbers of such stars. Furthermore, these objects are affected by an uncertain degree of reddening, because they tend to be fainter and more distant. Finally, the $(V-K)$ colour tends to saturate in metal-poor turnoff stars and is, hence, less sensitive to T_{eff} (see Fig. 9 of Ramírez & Meléndez 2005a). The discrepancy between T_{eff} determinations derived with the various methods does indicate that the effective temperature scale for metal-poor stars is still uncertain, and that a “hotter” temperature scale at low $[\text{Fe}/\text{H}]$ is not warranted. It is clear that further improvements in model atmospheres and line broadening theory, consideration of possible non-LTE effects on Balmer lines, and other factors will need to be explored in order to obtain fully consistent results. We estimate our temperatures to be determined within ± 100 K in an *absolute* sense. This uncertainty has a significant repercussion on the determination of the absolute carbon and oxygen abundances, and it is therefore important in the context of the interpretation of element ratios which are relevant to Galactic chemical evolution, such as C/Fe and O/Fe. On the other hand, the C/O ratio is hardly affected by systematic uncertainties in the T_{eff} scale, since the high-excitation C I and O I lines we employ show similar dependences on T_{eff} . A change in T_{eff} would affect the C and O abundances by comparable amounts, thereby preserving our final C/O estimates.

The derivation of the other atmospheric parameters (surface gravity, metallicity and microturbulence estimates) was also as described by Nissen et al. (2007). All atmospheric parameters were determined by iterating until consistency was achieved, with final adopted values as listed in Table 1. Gravities are derived from both *uvby*- β photometry and Hipparcos parallaxes, except in one case where neither was available.¹ Iron abundances were derived from Fe II lines, to take advantage of the relative insensitivity

¹ CD $-71^\circ 1234$, for which we derived $\log g$ by matching the difference between Fe I and Fe II abundances in the star with the average difference between the two sets of Fe abundances in the other stars.

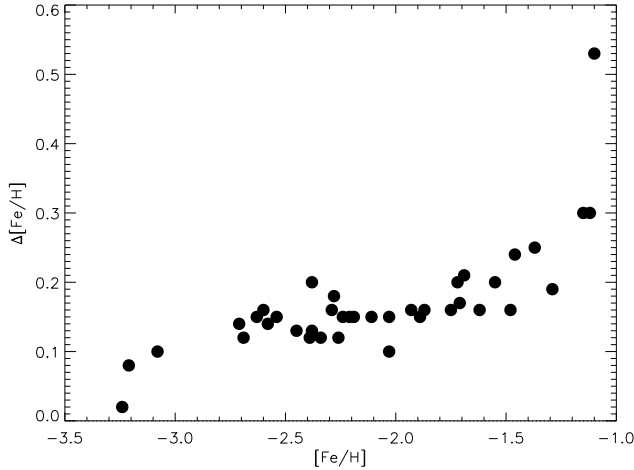


Fig. 3. $\Delta[\text{Fe}/\text{H}] = [\text{Fe}/\text{H}]_{\text{II}} - [\text{Fe}/\text{H}]_{\text{I}}$ (i.e., mean difference in the abundance of Fe as deduced from Fe II and Fe I lines) vs. $[\text{Fe}/\text{H}]_{\text{II}}$, for the stars with determinations from both ionization stages.

of such features to non-LTE effects (Asplund 2005). The statistical errors on the $[\text{Fe}/\text{H}]$ values are of the order of 0.05 – 0.10 dex. A number of unblended Fe I lines of similar strength as the Fe II lines were also measured in the UVES spectra, to check on the Fe I/Fe II ionisation equilibrium and on possible indications that non-LTE effects may have been underestimated. By comparing average abundances derived from lines in the two ionisation stages, we found that the residuals have a tendency to decrease with decreasing metallicity (see Fig. 3). The expectation is that non-LTE effects work in the sense of producing lower Fe abundance estimates from Fe I lines compared with Fe II (Asplund 2005). In our case, the average difference amounts to ~ 0.15 dex. The trend we find would point to differential, and metallicity-dependent, non-LTE effects for Fe I relative to the Sun, or to adopted values of T_{eff} which are too low (or possibly to a combination of both). The most metal-rich star in our sample (HD 193901) is the only one exhibiting a large disagreement between Fe I- and Fe II- based Fe abundances. This may be due to the fact that the Fe I abundance is based on only one line in HD 193901. Moreover, this line being quite strong, the abundance derived from it depends critically on the assumed microturbulence and damping constant. The $[\text{Fe}/\text{H}]$ values in Table 1 are based on the Fe II lines, relative to an adopted solar iron abundance of $\log \epsilon(\text{Fe})_{\odot} = 7.45$ (Asplund, Grevesse, & Sauval 2005).

As mentioned in Sect. 2, T_{eff} for the MIKE stars was determined from $\text{H}\alpha$ instead of $\text{H}\beta$. Taking into account that Nissen et al. (2007) found a systematic difference of 64 K between the T_{eff} scale based on $\text{H}\beta$ and the one based on $\text{H}\alpha$, we have thus transformed from the $T_{\text{eff}}(\text{H}\alpha)$ scale to the $T_{\text{eff}}(\text{H}\beta)$ scale accordingly. The other model atmosphere parameters were consistently derived as follows: (a) surface gravities from Stromgren photometry and Hipparcos parallax (only available for G84-29); (b) $[\text{Fe}/\text{H}]$ from the same Fe II lines as in Asplund et al. (2006).

The increase of T_{eff} by 64 K leads to a change of $[\text{Fe}/\text{H}]$ by +0.01 to +0.02 dex only. The corresponding change of $[\text{C}/\text{H}]$ and $[\text{O}/\text{H}]$ is -0.03 dex. Our choice of using $\text{H}\alpha$ in the

Table 2. The measured equivalent widths W_{λ} (in mÅ) for the C I and O I features detected in the 15 newly observed halo stars used in this study, together with the S/N near the features of interest. Only available online.

determination of T_{eff} for the MIKE spectra does not affect the deduced values of C/O and thus will not impact our final results (see also Fabbian et al. 2006). Note that in the case of G48-29, which was observed with both MIKE and UVES, there is good agreement between the atmospheric parameters estimated from the two sets of data (Table 1).

3.2. LTE abundance analysis

The equivalent widths of all lines measured in this study are listed in Table 2. The C I lines near 9100 Å, C I $\lambda 9405.7$, and the O I $\lambda\lambda 7772 - 7775$ triplet are all strong enough to be detected in our high-resolution, high S/N spectra for most stars, even at the lowest metallicities we explore. Akerman et al. (2004) used four high-excitation C I features (at 9061.4, 9078.3, 9094.8 and 9111.8 Å) to determine the carbon abundance. In addition to these lines, we also used C I $\lambda 9062.5$ and C I $\lambda 9088.5$ available in the same spectral region.² Furthermore, we analysed all our spectra to detect the relatively strong C I $\lambda 9405.7$ line (see Fig. 1). This line is comparable in strength to C I $\lambda 9094.8$ (the strongest in the 9100 Å group), the difference in excitation potentials being almost compensated by the difference in oscillator strengths (values are taken from Wiese, Fuhr, & Deters 1996, as retrieved using the NIST Atomic Spectra Database version 3³). It is thus still detected at the lowest metallicities ($[\text{Fe}/\text{H}] \lesssim -3$). We found no indications of systematic differences in the carbon abundance deduced from these additional C I transitions compared with those used by Akerman et al. (2004); by including measurements of more C I lines in our analysis, we improved the accuracy of the determination of the carbon abundance, especially at the lowest metallicities. Although only three O I lines were analysed, they have the advantage of falling in a spectral region which is free of contamination by telluric absorption.

In the star LP831-70, which was observed with MIKE, we could not detect with confidence any carbon or oxygen line, despite the relatively high S/N achieved. Taking for comparison the very metal-poor star CD-24 17504, where the stronger C I and O I lines are detected in the UVES spectra, we find that LP831-70 is cooler and less metal-poor. While the cooler temperature goes in the direction of making the C I and O I features weaker, the non-detections of the C I and O I lines are still surprising, given its higher metallicity (by about a factor of two).

In general, the accuracy of the equivalent widths measurements is about ± 1 mÅ (1σ), estimated empirically by

² For C I $\lambda 9088.5$, we confirmed via spectral synthesis that its blending with a weak Fe I line (at 9088.3 Å) should not be neglected in the measurement of its equivalent width and we have therefore taken it into account.

³ Available online at: <http://physics.nist.gov/PhysRefData/ASD/index.html>

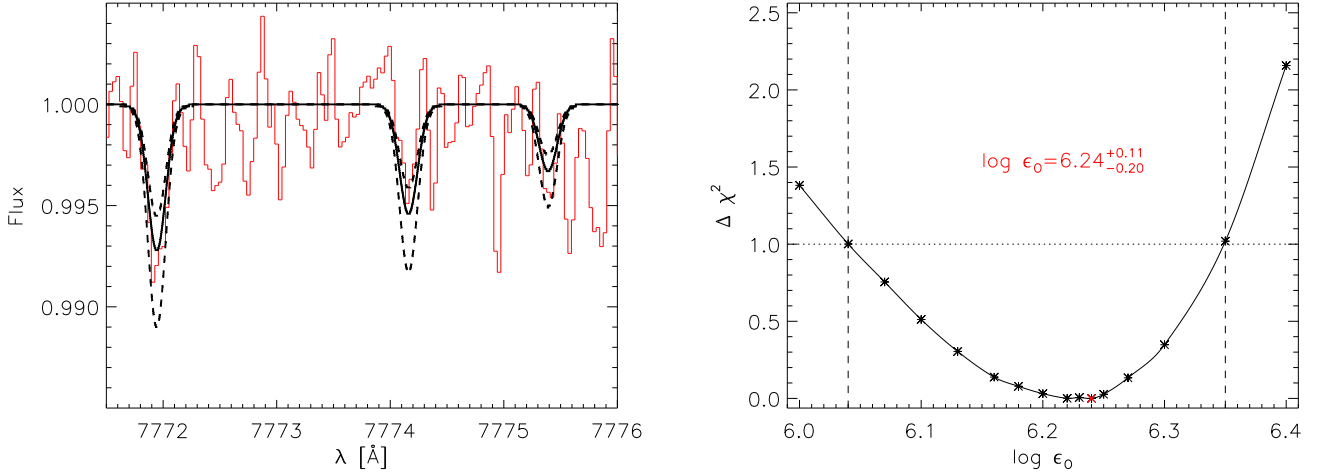


Fig. 4. The spectrum synthesis of the O I IR triplet in the star CD-24 17504, for different oxygen abundances. A gaussian convolution profile with macroturbulence and instrumental broadening of 5 km s^{-1} was adopted. *Left panel:* observed (thin) and computed (thick) line profiles. The latter are for our best estimate of the oxygen abundance (solid) and $\pm 1 - \sigma$ (dashed), i.e. corresponding to $\log \epsilon_{\text{O}} = 6.24^{+0.11}_{-0.20}$. *Right panel:* chi square variation (solid curve) and corresponding $1 - \sigma$ uncertainties (dashed vertical lines).

comparing the values measured on different spectra of the same star, or from adjacent orders within the same spectrum (e.g. the O I triplet lines in our UVES observations). The equivalent widths listed in Table 2 were employed to perform the LTE abundance analysis through the use of the “Uppsala package” code EQWIDTH and of MARCS model atmospheres, deriving, for each star in the sample, the metallicity $[\text{Fe}/\text{H}]$ and the LTE C and O abundances. The line-to-line scatter in the abundances we obtain for carbon and oxygen is small (typically less than ± 0.05 dex); at low $[\text{Fe}/\text{H}]$ the main source of error is the uncertainty in the equivalent widths of weak lines. An uncertainty of $\pm 1 \text{ m\AA}$ in W_{λ} translates to a random error of approximately 15% in the abundances of C and O in the most metal-poor stars.

CD-24 17504 (alias G275-4) was a special case. This star has the lowest metallicity ($[\text{Fe}/\text{H}] = -3.21$) among those in the new sample where we detect carbon lines. As can be seen from Fig. 4, the O I lines are also very weak and almost at the level of the noise—we detect with certainty only the bluest and strongest transition of the O I triplet, $\lambda 7771.9$, with an equivalent width $W_{\lambda} = 1.7 \text{ m\AA}$. In order to put more reliable limits on the oxygen abundance (and, thus, on $[\text{C}/\text{O}]$) in this star, we carried out a spectral synthesis of the O I triplet with the “Uppsala package” code BSYN for a range of values of the oxygen abundance. We then performed a chi-square minimization between the observed and synthesised spectra for the wavelength region comprising the triplet lines, to find the best estimate of the oxygen content of this star (see right-hand panel of Fig. 4). The LTE result is $\log \epsilon_{\text{O}} = 6.24^{+0.11}_{-0.20}$, implying $[\text{C}/\text{O}] = -0.16$.

In general, the LTE abundances we derive seem to signal high values of up to $[\text{C}/\text{O}] \sim -0.2$ at the very lowest metallicities. In the following section, we apply non-LTE corrections computed specifically for the stars in the sample, and for each of the lines we have analysed, in order to assess the reality of the upturn in $[\text{C}/\text{O}]$ at low values of $[\text{O}/\text{H}]$ suggested by the LTE abundances. By accounting for non-LTE effects in the formation of the spectral lines of

interest, we remove one of the main sources of systematic error, although there are still residual uncertainties in the atomic (in particular, collision) data used in the non-LTE analysis.

3.3. C I and O I line formation: non-LTE abundance corrections calculations

The C I and O I spectral features used here are affected by departures from LTE. Therefore, it is important to account for non-LTE effects in order to derive reliable estimates of the abundances of carbon and oxygen. Not only is it important to understand how these effects work differentially between lines of the same element, but in our case we obviously need to understand how the different non-LTE corrections affect the behaviour of $[\text{C}/\text{O}]$ vs. $[\text{O}/\text{H}]$ which is the main goal of this work.

Our recent investigations of C and O (Fabbian et al. 2006, 2008a) have uncovered larger deviations from LTE for the O I lines than for the C I lines. In Fabbian et al. (2006), we performed detailed non-LTE calculations for the carbon lines which are employed also in the present work. For the oxygen non-LTE corrections, in Fabbian et al. (2006) we assumed the estimates by Akerman et al. (2004) for all but the five most metal-poor sample stars, for which we re-estimated larger non-LTE abundance corrections. Such preliminary investigation on the oxygen triplet subsequently led to the work presented in Fabbian et al. (2008a), in which we additionally introduced quantum-mechanical estimates for electron-impact excitation. As discussed in Fabbian et al. (2008a), due to their importance in coupling atomic levels of interest and thus forcing large level overpopulation due to flow from radiatively pumped O I resonance lines, these new collisional data give much larger non-LTE corrections for metal-poor turnoff stars, which we

adopted here. Unfortunately, no such quantum-mechanical calculations are as yet available for carbon.⁴

Regarding the poorly known cross-sections for H collisions, while they do not have a large impact on the C I non-LTE corrections found in Fabbian et al. (2006) which we adopt here, and which amount to ~ -0.4 dex in halo turnoff stars at $[\text{Fe}/\text{H}] \sim -3$, they are likely the largest single remaining cause of uncertainty in the oxygen non-LTE calculations. The results in Fabbian et al. (2008a) show that neglecting collisions with neutral H atoms leads to the negative abundance corrections becoming more severe (by up to ~ 0.4 dex). Since oxygen is so sensitive to the choice of H collision efficiency, in the absence of detailed quantum-mechanical calculations, one may look for indirect evidence as to whether the classical recipe by Drawin (1968, 1969) usually employed needs to be scaled by large factors. As discussed in Fabbian et al. (2008a), while some high scaling factors have been suggested in the literature, we believe that the Drawin recipe may indeed be a fairly accurate approximation for oxygen, based on evidence in the Sun and from the fact that derived $[\text{O}/\text{Fe}]$ ratios would become unreasonably low and close to solar at low metallicity if H collisions were neglected. The resulting oxygen non-LTE corrections are then typically ~ -0.5 dex for metal-poor turnoff stars. Non-LTE effects on the C I and O I lines thus work differentially at low metallicity, giving higher $[\text{C}/\text{O}]$ ratios by $\sim +0.1$ dex compared to LTE.

4. Results

Our final abundance results are given in Table 3. Figures 5 and 6 show the corresponding trends of $[\text{C}/\text{Fe}]$ and $[\text{O}/\text{Fe}]$ with $[\text{Fe}/\text{H}]$, while Figs. 7 and 8 show the behaviour of $[\text{C}/\text{O}]$ and $[\text{Fe}/\text{O}]$ with $[\text{O}/\text{H}]$.

The typical errors associated with our abundance estimates for the most metal-poor stars in the sample (where the uncertainties are largest due to fewer and weaker C I and O I lines being measured) are indicated by the error bars in the lower left-hand corner of Figs. 5, 6, 7 and 8. They correspond to the statistical error introduced by the $1 - \sigma$ errors in T_{eff} (± 100 K), $\log g$ (± 0.15 dex), microturbulence (± 0.3 km/s) and equivalent width. In particular, the latter measurement errors dominate for the most metal-poor stars. The uncertainty on T_{eff} is significant too, in the case of C/Fe and O/Fe, but cancels out in the case of C/O.

Referring to Fig. 5, it is interesting to note that the introduction of non-LTE corrections in the analysis of the C I

lines completely erases the LTE trend of increasing $[\text{C}/\text{Fe}]$ with decreasing $[\text{Fe}/\text{H}]$. The essentially flat behaviour of $[\text{C}/\text{Fe}]$ at near-solar values over three orders of magnitude in $[\text{Fe}/\text{H}]$ seen in the lower panel of Fig. 5 would indicate that C and Fe production in the Galaxy has proceeded on similar timescales and thus presumably from similar sources.

Regarding the widely debated behaviour of $[\text{O}/\text{Fe}]$ at low metallicity, our non-LTE corrected abundances (Fig. 6) seem to back the idea that the real trend may be essentially flat, with abundances derived from the O I 7772 – 7775 Å triplet lying much closer than often reported to those usually derived in the literature from $[\text{O I}]$ and infrared OH lines. When accounting for full 3D non-LTE effects on *all* the affected lines becomes possible, it is quite plausible that agreement may be finally reached. At this stage, we can only comment on the fact that the application of non-LTE corrections without taking into account H collisions seems to overcorrect the LTE abundances and yield values of $[\text{O}/\text{Fe}]$ which are almost certainly too low, being close to solar at $[\text{Fe}/\text{H}] \lesssim -2.5$ (see Fig. 6). We consider it more likely that H collisions are fairly efficient in the case of oxygen, making the relevant non-LTE corrections less severe and only slightly larger than for carbon. In addition, based on the results of solar observations by Allende Prieto et al. (2004), we can safely rule out that LTE ($S_{\text{H}} \gg 1$) applies to the O I 7772 – 7775 Å triplet. It remains of high priority to carry out full non-LTE calculations with hydrodynamical model atmospheres for oxygen at low metallicity, hopefully including future quantum-mechanical calculations of inelastic H collisions.

Turning now to the $[\text{C}/\text{O}]$ ratio, non-LTE results for our sample are shown in Fig. 7, for two different choices of S_{H} , together with those for higher-metallicity disc stars obtained by Bensby & Feltzing (2006) from forbidden C I and O I lines. The new data strengthen the suggestion by Akerman et al. (2004) that the decrease of $[\text{C}/\text{O}]$ between solar and intermediately-low metallicities (i.e., the metallicity range of thin and thick disc), reaching a minimum of $[\text{C}/\text{O}] \sim -0.7$ at $[\text{O}/\text{H}] \sim -1.0$ in our data, turns into an *increase* in halo stars of even lower metallicities. The adoption of non-LTE corrections tends to move the data points for the metal-poor halo stars to: (a) much lower values of $[\text{O}/\text{H}]$ due to large oxygen non-LTE corrections, and (b) to higher $[\text{C}/\text{O}]$ values because the negative non-LTE corrections are 0.1 – 0.4 dex more severe for oxygen than for carbon, depending on the choice of H collision efficiency and on the particular stellar parameters. This “stretches” the rising trend seen in LTE towards lower metallicities, while at the same time raising $[\text{C}/\text{O}]$ to close-to-solar values. The rise has a slope of ~ -0.3 in the $[\text{C}/\text{O}]$ vs. $[\text{O}/\text{H}]$ plane.

⁴ Collisions with electrons may indeed be the most urgent outstanding problem to be addressed in the formation of the C I lines, since including H collisions only affects those features by $\lesssim 0.1$ dex for typical stellar parameters of interest. Given the similarity in the atomic structure, one may expect that the C I IR lines are also significantly affected by intersystem collisional coupling, and that the quantum-mechanical electron-impact rates are larger than the current estimates, as found in the case of oxygen. Our tests on carbon indeed indicate a significant sensitivity to electron collisions, including between singlet and triplet systems in the atom, but especially to the ground state. However, an increase in such rates tends to weaken the line, therefore *reducing* the non-LTE effect on C I. We then expect that the high $[\text{C}/\text{O}]$ values we find in this work may be further increased, should more efficient electron collisions be adopted for carbon too.

We have included in Fig. 7 the $[\text{C}/\text{O}]$ measurements in metal-poor DLAs by Pettini et al. (2008) which seem to match well the values deduced here in halo stars of similar $[\text{O}/\text{H}]$. The good agreement in the $[\text{C}/\text{O}]$ ratios measured in different astrophysical environments and at different epochs strengthens the interpretation that carbon was somehow overproduced in early stages of galactic chemical evolution. On the other hand, the halo giants considered by Spite et al. (2005) (we refer here to the “unmixed” objects from their sample) appear to have generally lower $[\text{C}/\text{O}]$ values than those derived here, particularly in view of the large 3D effects which are likely to apply, in giants, to the CH features employed in their analysis (Collet et al. 2007). Such

Table 3. Derived abundances of oxygen and carbon for the sample of 43 halo stars. The resulting [C/H], [O/H] and [C/O] abundance ratios derived in this study are also given, both for LTE and non-LTE (using our adopted abundance corrections obtained with and without including collisions with H I atoms, respectively). In the non-LTE case, S_H indicates the scaling factor regulating the efficiency of the collisions with neutral H atoms via the Drawin formula. The differential abundances ([C/O], [O/H], [Fe/H]) with respect to the Sun were derived assuming¹ $\log(C/H)_\odot + 12 = 8.39$, $\log(O/H)_\odot + 12 = 8.66$, and $\log(Fe/H)_\odot + 12 = 7.45$.

ID	$\log \epsilon_C$ (LTE)	$\log \epsilon_O$ (LTE)	[C/H] (LTE)	[C/H] ($S_H = 0$)	[C/H] ($S_H = 1$)	[O/H] (LTE)	[O/H] ($S_H = 0$)	[O/H] ($S_H = 1$)	[C/O] (LTE)	[C/O] ($S_H = 0$)	[C/O] ($S_H = 1$)
UVES (2001)											
BD-13°3442	6.14	6.89	-2.25	-2.62	-2.56	-1.77	-2.39	-2.11	-0.48	-0.23	-0.45
CD-30°18140	6.73	7.58	-1.66	-1.93	-1.84	-1.08	-1.27	-1.22	-0.58	-0.66	-0.62
CD-35°14849	6.38	7.05	-2.01	-2.30	-2.22	-1.61	-1.99	-1.81	-0.40	-0.31	-0.41
CD-42°14278	6.54	7.28	-1.85	-2.07	-1.97	-1.38	-1.55	-1.47	-0.47	-0.52	-0.50
G011-044	6.58	7.37	-1.81	-2.03	-1.94	-1.29	-1.47	-1.40	-0.52	-0.56	-0.54
G013-009	6.48	7.19	-1.91	-2.25	-2.17	-1.47	-1.83	-1.73	-0.44	-0.42	-0.44
G018-039	7.23	8.04	-1.16	-1.40	-1.29	-0.62	-0.84	-0.77	-0.54	-0.56	-0.52
G020-008	6.54	7.30	-1.85	-2.11	-2.01	-1.36	-1.63	-1.51	-0.49	-0.48	-0.50
G024-003	6.65	7.56	-1.74	-1.97	-1.87	-1.10	-1.30	-1.24	-0.64	-0.67	-0.63
G029-023	6.82	7.71	-1.57	-1.84	-1.75	-0.95	-1.16	-1.11	-0.62	-0.68	-0.64
G053-041	7.01	7.78	-1.38	-1.66	-1.53	-0.88	-1.09	-1.03	-0.50	-0.57	-0.50
G064-012	5.67	6.45	-2.72	-3.17	-3.09	-2.21	-3.10	-2.71	-0.51	-0.07	-0.38
G064-037	5.71	6.42	-2.68	-3.13	-3.05	-2.24	-3.12	-2.70	-0.44	-0.01	-0.35
G066-030	6.91	7.90	-1.48	-1.76	-1.66	-0.76	-1.03	-0.96	-0.72	-0.73	-0.70
G126-062	6.94	7.86	-1.45	-1.72	-1.62	-0.80	-1.04	-0.98	-0.65	-0.68	-0.64
G186-026	6.15	6.75	-2.24	-2.56	-2.49	-1.91	-2.47	-2.20	-0.33	-0.09	-0.29
HD106038	7.38	8.05	-1.01	-1.28	-1.14	-0.61	-0.82	-0.75	-0.40	-0.46	-0.39
HD108177	6.90	7.75	-1.49	-1.73	-1.63	-0.91	-1.11	-1.04	-0.58	-0.62	-0.59
HD110621	7.02	7.89	-1.37	-1.65	-1.54	-0.77	-0.99	-0.94	-0.60	-0.66	-0.60
HD140283	6.27	6.99	-2.12	-2.40	-2.32	-1.67	-1.91	-1.81	-0.45	-0.49	-0.51
HD160617	6.71	7.39	-1.68	-1.97	-1.87	-1.27	-1.47	-1.42	-0.41	-0.50	-0.45
HD179626	7.54	8.38	-0.85	-1.11	-0.98	-0.28	-0.51	-0.45	-0.57	-0.60	-0.53
HD181743	6.76	7.58	-1.63	-1.84	-1.74	-1.08	-1.24	-1.18	-0.55	-0.60	-0.56
HD188031	6.84	7.69	-1.55	-1.81	-1.72	-0.97	-1.18	-1.12	-0.58	-0.63	-0.60
HD193901	7.41	8.17	-0.98	-1.19	-1.06	-0.49	-0.65	-0.58	-0.49	-0.54	-0.48
HD194598	7.44	8.15	-0.95	-1.22	-1.11	-0.51	-0.75	-0.68	-0.44	-0.47	-0.43
HD215801	6.32	7.22	-2.07	-2.37	-2.29	-1.44	-1.72	-1.61	-0.63	-0.65	-0.68
LP815-43	6.16	6.71 ^a	-2.23	-2.63	-2.56	-1.95	-2.70	-2.36	-0.28	+0.07	-0.20
UVES (2004)											
CD-24 17504 ^b	5.81	6.24	-2.58	-2.91	-2.84	-2.42	-3.25	-2.87	-0.16	+0.34	+0.03
CD-71 1234	6.28	7.03	-2.11	-2.40	-2.33	-1.63	-2.04	-1.86	-0.48	-0.36	-0.47
CS 22943-0095	6.56	7.33	-1.83	-2.13	-2.05	-1.33	-1.66	-1.52	-0.50	-0.47	-0.53
G004-037	6.26	7.16	-2.13	-2.44	-2.36	-1.50	-1.96	-1.75	-0.63	-0.48	-0.61
G048-029 ^c	6.01	6.81	-2.38	-2.70	-2.64	-1.85	-2.48	-2.18	-0.53	-0.22	-0.46
G059-027	6.81	7.60	-1.58	-1.84	-1.74	-1.06	-1.24	-1.18	-0.52	-0.60	-0.56
G126-052	6.42	7.15	-1.97	-2.26	-2.18	-1.51	-1.83	-1.69	-0.46	-0.43	-0.49
G166-054	6.03	6.91	-2.36	-2.72	-2.64	-1.75	-2.33	-2.05	-0.61	-0.39	-0.59
HD84937	6.53	7.27	-1.86	-2.15	-2.07	-1.39	-1.64	-1.56	-0.47	-0.51	-0.51
HD338529	6.46	7.24	-1.93	-2.25	-2.17	-1.42	-1.77	-1.63	-0.51	-0.48	-0.54
LP635-014	6.39	7.06	-2.00	-2.33	-2.25	-1.60	-2.03	-1.85	-0.40	-0.30	-0.40
LP651-004	6.08	7.04	-2.31	-2.99	-2.58	-1.62	-2.21	-1.93	-0.69	-0.44	-0.65
MIKE (2003)											
G041-041	5.96	6.74	-2.43	-2.85	-2.76	-1.92	-2.54	-2.25	-0.51	-0.31	-0.51
G048-029 ^c	6.11	6.80	-2.28	-2.66	-2.59	-1.86	-2.50	-2.20	-0.42	-0.16	-0.39
G084-029	6.06	6.87	-2.33	-2.72	-2.63	-1.79	-2.33	-2.08	-0.54	-0.39	-0.55
LP831-070 ^b	< 5.77	< 6.53	< -2.62	< -3.01	< -2.93	< -2.13	< -2.95	< -2.54	-	-	-

¹ Asplund, Grevesse, & Sauval 2005.

^a As discussed by Fabbian et al. (2006), the oxygen determination by Nissen et al. (2002) for this stars is more reliable than that derived from the UVES 2001 spectra and was therefore adopted here.

^b Since the O I lines are barely visible in these two stars, spectral synthesis and chi square minimization (see text) of the profiles of the O I triplet lines were used in order to constrain their oxygen content.

^c This star was observed in both UVES (2004) and MIKE (2003) runs. The C and O abundances derived in the two cases using the respective atmospheric parameters for the two sets of spectra are shown here, while their mean was adopted in Figs. 5, 6, 7 and 8.

corrections would decrease their [C/O] determinations by several tenths of a dex.

Further investigations targeting stars at different evolutionary stages are bound to help shed light on this issue. The star with the highest [C/O] in our sample is

CD-24 17504, for which we deduce $[Fe/H] = -3.21$, and $[C/O] = +0.03$ or $+0.34$, depending on whether the effects of H collisions are included or not. Richard, Michaud & Richer (2002) specifically discuss this star as peculiar in relation to atomic diffusion effects, arguing that these

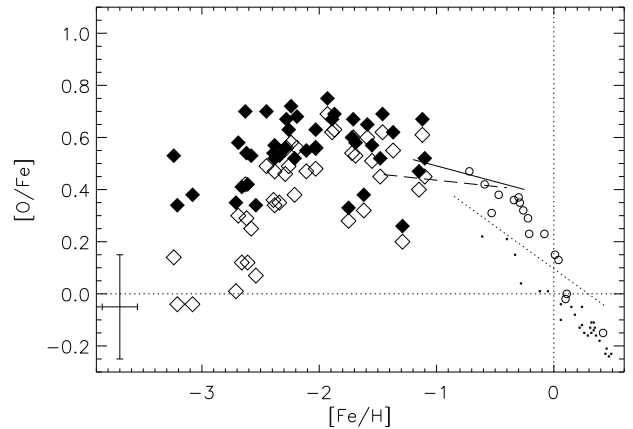
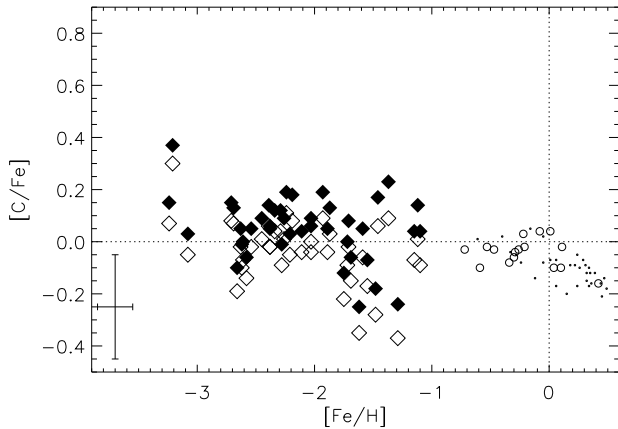
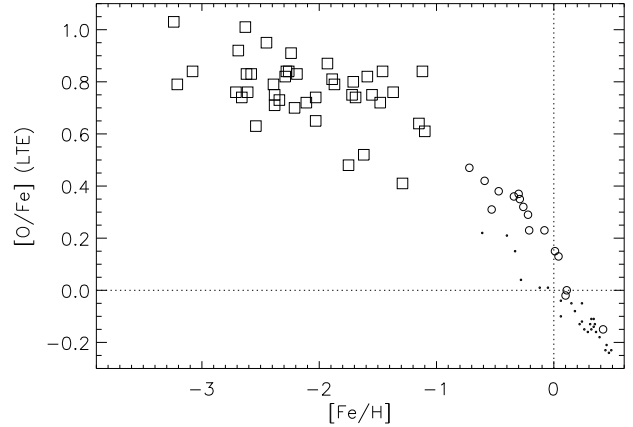
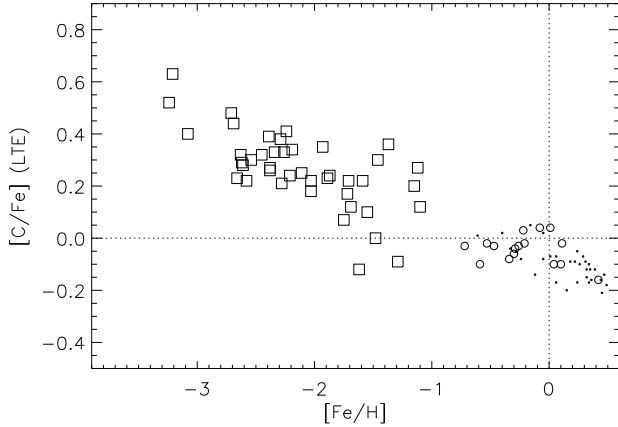


Fig. 5. Runs of $[C/Fe]$ versus $[Fe/H]$ for our sample stars, respectively in LTE (upper panel) and non-LTE (lower panel): filled diamonds = H collisions ‘à la Drawin’; empty diamonds = no H collisions). The results by Bensby & Feltzing (2006), obtained from $[C\text{I}]$ and $[O\text{I}]$ lines free from non-LTE effects, are additionally shown for thin (small dots) and thick (open circles) disc stars. The dotted horizontal and vertical lines indicate the solar values.

Fig. 6. Runs of $[O/Fe]$ versus $[Fe/H]$ in LTE (upper panel) and non-LTE (lower panels), respectively. Symbols are as in Fig. 5. Lines in the bottom panel show the fits derived by Ramírez et al. (2006) to their $[O/Fe]$ data, separately for thin disc (dotted line), thick disc (solid line) and halo (dashed line) stars.

could have modified its relative metal abundances, so that caution should be exercised when interpreting its derived abundance ratios in terms of nucleosynthesis. In particular, their Figs. 5 and 11 show that differential effects on C and O may be important, mainly due to larger oxygen surface abundance decrease.

The other two stars with metallicities below $[Fe/H] = -3$ (G64-12 and G64-37 from the Akerman et al. 2004 sample) have lower carbon enhancements with $[C/O] \sim -0.35$ or ~ 0 , again depending on whether H collisions are included or not. In the case of LP831-70 ($[Fe/H] = -2.94$), our spectrum is too noisy for positive detections of the weak $C\text{I}$ and $O\text{I}$ lines. Our conservative upper limits (Tables 2 and 3) suggest that this star has lower C and O abundances than other stars of similar metallicity.

Finally, we show the trend of $[Fe/O]$ with $[O/H]$ in Fig. 8. It is interesting to compare this diagram with Fig. 7. If carbon and iron were produced mainly by stars with similar evolutionary timescales, one would expect the figures to look very similar, as indeed they do.

5. Galactic chemical evolution of carbon and oxygen

Stars born at early galactic epochs and living through to the present time bear the signatures in their chemical composition (in particular in the relative abundances of different elements as a function of metal content) of events occurring during the history of the Milky Way, providing information on its different formation events (Freeman & Bland-Hawthorn 2002) and on the nucleosynthetic channels that build the various elements in the interiors of stars.

While it is known that carbon is produced during helium burning in stars of all masses, the sites of major contribution to the C enrichment in our Galaxy and the dependence of yields on stellar mass, which is used as input to Galactic Chemical Evolution (GCE) models describing how the abundances of various elements vary in time, are not yet agreed upon. The roughly flat $[C/Fe]$ trend we see down to low metallicities seems to suggest that the sources of carbon and iron have similar timescales, at least until the metallicity becomes extremely low. At variance with the case of oxygen, stars of different masses and thus operating on different timescales have contributed to the build-

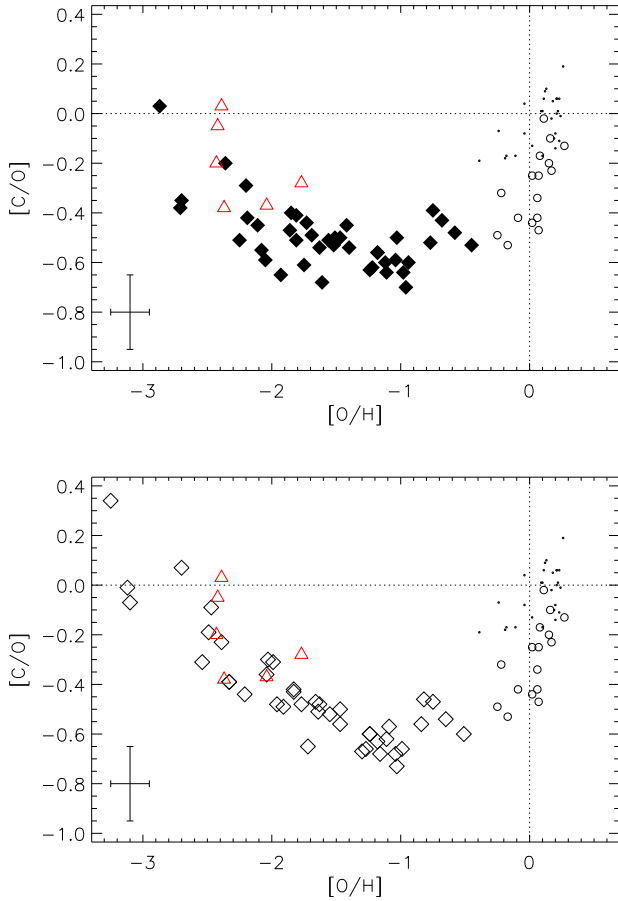


Fig. 7. Final estimates of $[C/O]$ versus $[O/H]$ for our sample stars using, for both carbon and oxygen, $S_H = 1$ (upper panel), or neglecting H collisions altogether (lower panel). The meaning of the symbols for the different Galactic stellar components is as in Fig. 5, lower panel. The data indicated by triangles are the values measured in metal-poor damped Lyman alpha systems at high redshifts by Pettini et al. (2008).

up of carbon during the Galaxy’s history. Standard GCE models predict that the time lag between the prompt ISM enrichment of oxygen due to short-lived massive stars exploding as type II supernovae, and the delayed released of carbon, should cause C/O to constantly decrease with decreasing metallicity. In particular, Carigi et al. (2005) have suggested that yields from massive stars are the overwhelming source of carbon at early stages, while later on, at the end of their slower evolution, low- and intermediate-mass stars would be able to contribute carbon ejecta into the ISM in a comparable amount. In their models, a combination of sources differing in mass and thus contributing at different times is required to match the observed trends. In contrast, Gavilán, Buell & Mollá (2005) have argued that low- and intermediate-mass stars alone may account for the carbon evolution.

Given the very low metal-content of most stars in our sample, with oxygen abundances as low as 10^{-3} of the solar value, these objects are presumably associated with very early star formation in our Galaxy, before the end of the halo build-up. Thus, by being the only survivors to

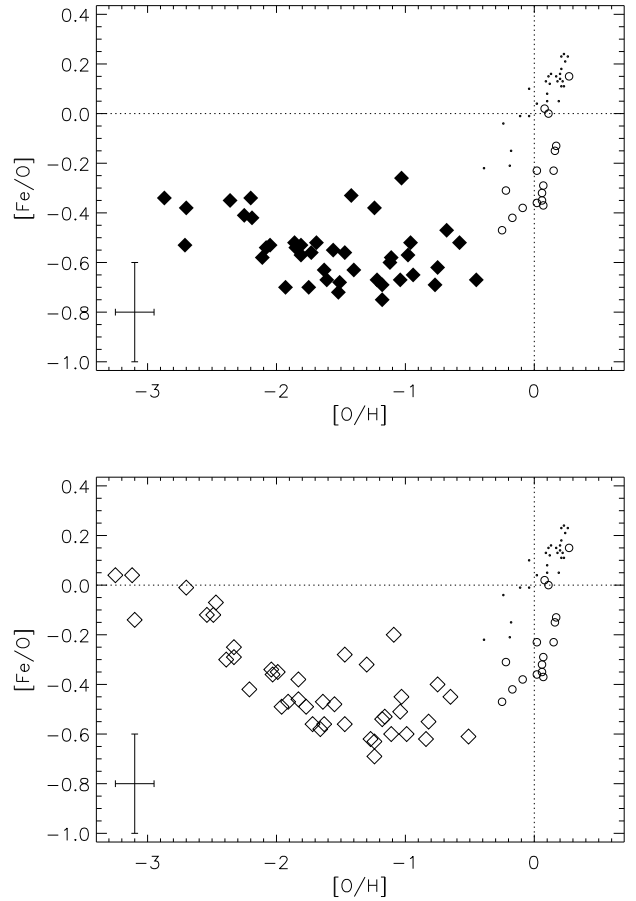


Fig. 8. Final estimates of $[Fe/O]$ versus $[O/H]$ for our sample stars, using for oxygen either $S_H = 1$ (upper panel) or neglecting H collisions altogether (lower panel). The meaning of the symbols for the different Galactic stellar components is as in Fig. 5, lower panel.

the present, they provide a window on nucleosynthetic processes taking place in the stars that have existed at such early times. A straightforward interpretation of the high C/O values we find at low metallicities is that the first episodes of star formation in the Galaxy provided a source of high C abundance, perhaps thanks to a primordial generation of massive, zero-metallicity stars. According to current theoretical models describing the yields of these hypothetical objects, it is plausible that they could have indeed contributed large C yields (e.g. Chieffi & Limongi 2002, 2004).

Akerman et al. (2004) constructed GCE models in order to interpret their tentative discovery of a $[C/O]$ rise at low metallicity. By adopting the Population III yields of Chieffi & Limongi (2002), they could reproduce the observed behaviour, in particular when using a top-heavy IMF. This would imply, as assumed in the derivation of those yields, that the nucleosynthetic channel $^{12}C(\alpha, \gamma)^{16}O$ proceeds at a lower rate in such primordial objects.

Chiappini et al. (2006) on the other hand argue that the $[C/O]$ upturn can be explained through fast stellar rotation at very low metallicities, so that due to lower average core temperature, the conversion of C into O would be less efficient. However, they also make it clear that it is not granted

that the high C/O values should necessarily imply the signature of massive Pop. III stars, since their own results can be achieved without including zero-metallicity yields.

Carigi et al. (2005) successfully fitted the observed radial gradients of C/O and O/H in the Milky Way with models which use a steep IMF and in which the relative proportions of carbon released into the interstellar medium by massive stars on the one hand, and low- and intermediate-mass stars on the other, vary with time and galactocentric distance. Their models are in reasonably good agreement with the observed trends of the ratios [C/O], [C/Fe] and [O/Fe] reported here.

Nissen et al. (2007) reported evidence for an increase in the abundance of Zn relative to Fe at the lowest metallicities, with $[Zn/Fe] \simeq +0.5$ at $[Fe/H] \lesssim -3$. Traditional yields of Type II SNe (Nomoto et al. 1997) cannot reach the high observed $[Zn/Fe]$ values, which instead seem to require either the ejecta of Population III hypernovae, or high Zn production from core-collapse, very massive ($M \sim 500\text{--}1000 M_{\odot}$) stars (Ohkubo et al. 2006).

Kobayashi et al. (2006) calculated yields for a wide range of metallicities ($Z = 0 - Z_{\odot}$) and explosion energies, including hypernovae. Their predicted [C/Fe]–[Fe/H] and [O/Fe]–[Fe/H] relations seem to match our derived abundances for halo stars (assuming $S_H = 0$ and 1 for carbon and oxygen respectively) fairly closely. In particular for carbon, the agreement seems to indicate that enrichment from stellar winds and the contribution of low- and intermediate-mass stars are not important for this element at low metallicity, since those are not included in the calculations by Kobayashi et al. (2006). Those authors pointed out that in order to explain simultaneously the high C abundances observed in extremely metal-poor stars and the supersolar Zn/Fe ratios at low metallicities, other enrichment sources (e.g. a few Pop. III supernova explosions in the very early inhomogeneous intergalactic medium, or external enrichment from a binary companion) are needed. The final C yields may in fact turn out to be even higher than predicted by Kobayashi and collaborators, if winds of massive stars at very low metallicity contribute significant additional amounts of carbon.

Finally, Smiljanic et al. (2008) very recently discussed possible signatures of hypernova nucleosynthesis in HD 106038, one of the stars in our sample, for which we derive $[Fe/H] = -1.37$. Even though their hypothesis is mainly based on very large beryllium enhancement, they also discuss available literature values for other elements. For carbon and oxygen in this star, we find $[C/Fe] = +0.23/+0.09$ and $[O/Fe] = +0.62/+0.55$, depending on whether H collisions are included or not. The values of [O/Fe] we deduce are in good agreement with the non-LTE determination by Meléndez et al. (2006) of $[O/Fe] = +0.56 \pm 0.10$.

6. Conclusions

We have presented non-LTE corrected element abundances in a sample of 43 metal-poor halo stars, and carried out the most extensive study to date of the relative abundances of carbon and oxygen as a function of metallicity. Updated estimates of stellar parameters for stars with $[Fe/H] < -1$ in the sample of Akerman et al. (2004) were derived consistently with the rest of our sample stars following Nissen et al. (2007). Akerman et al. (2004) estimated that, to a

first approximation, non-LTE and 3D effects on the formation of the C I and O I lines they analysed are of similar magnitude so that their neglect should not lead to a systematic bias in the values of [C/O] deduced. However, they also warned that a quantitative assessment of non-LTE effects was required to confirm the reality of their tentative findings. Here we have included non-LTE corrections for both C and O and considered additional C I lines; taken together these two aspects of the present work represent significant improvements over earlier published studies by reducing both systematic and statistical uncertainties in the determinations of the C and O abundances. The sample of stars analysed by Akerman et al. (2004) was subsequently used by Meléndez et al. (2006) in their study of oxygen at low metallicity. However, while Meléndez and collaborators applied their non-LTE corrections directly to published values, we have re-derived the abundances to complement our sample of newly observed stars in a consistent fashion. Our main findings are as follows.

1. After accounting for large negative non-LTE effects on the C I and O I lines employed here, our resulting abundances reinforce and place on stronger footing the case for a trend of rising [C/O] with decreasing [O/H] in Galactic halo stars first discovered by Akerman et al. (2004). Our improved analysis finds the strongest evidence so far for an increase in [C/O] at $[O/H] \lesssim -2$. This seems to add to the suggestion that high [C/O] values are commonplace at low metallicities, as recently argued by Pettini et al. (2008) in their investigation of high-redshift absorption systems.
2. The exact magnitudes of the corrections to the abundances of C and O from non-LTE effects are still uncertain because of poorly known H collisions, especially for oxygen. The non-LTE effects on the C I and O I lines we have analysed are both negative and thus affect less the determination of the [C/O] ratio than the individual abundances of the two elements. However, the effects do not cancel out completely, with the corrections for the O I lines being larger than those for the C I lines in the low-metallicity regime we are most interested in. Consequently, consideration of non-LTE effects leads to residual *positive* corrections to the values of [C/O] compared to LTE analyses which tend to *underestimate* [C/O].
3. While detailed 3D corrections are not available, we do not expect them to change our results for [C/O] much, because determination of this ratio from high excitation C I and O I lines is virtually insensitive to temperature changes in the atmospheric model structure, and because 3D abundance corrections for these lines are expected to be small, of the same sign, and of similar magnitude, and should therefore cancel out to a large extent in the derivation of [C/O]. There may of course be some complicated differential effects due to the coupling between non-LTE and 3D. Full 3D non-LTE computations at very low metallicity using the new generation of hydrodynamical model atmospheres and addressing this remaining uncertainty are beyond the scope of this paper. However, given the important role in galactic chemical evolution, targeting these elements remains a priority for future investigations.
4. We find that the [C/O] ratio reduces by a factor of 3–4 when [O/H] decreases from solar to $\sim 1/10$ solar (as

already shown e.g. by Gustafsson et al. 1999 and as predicted by GCE models due mainly to metallicity-dependent theoretical carbon yields from winds/mass loss in metal-rich massive stars). At still lower metallicities, [C/O] tends to increase—with a slope of ~ -0.3 in the [C/O] vs. [O/H] plane—reaching near-solar values again at [O/H] ~ -3 .

Our results likely signal non-standard carbon and/or oxygen nucleosynthesis, offering potentially crucial clues on the early history of the Milky Way. Massive Population III stars may be the sources responsible for such high [C/O] ratios, with large carbon yields from a generation of (so far elusive) primordial, massive, metal-free objects. Alternatively, Population II stars in which high production of C may have been aided by strong mass loss induced by fast rotation could also be called upon to explain our results. Models of fast-rotating, massive stars (so called “spin-stars”) developed recently (Meynet et al. 2007) may provide an explanation to our observations. Implications in terms of early generations of stars at low metallicity including more fast-rotators than in the present Universe will need to be confirmed by future observational and theoretical studies.

Acknowledgements. DF acknowledges the hospitality of the Department of Physics and Astronomy of the University of Aarhus, Denmark. We are grateful to Jorge Meléndez for fruitful discussions on the [O/Fe] ratio and for advice on the IRFM temperature scale, and to Anna Frebel for her help in estimating colour excesses and for sharing updated C and O abundance estimates in HE 1327 2326 in advance of publication. We also thank Kurt Adelberger for the observations with the Magellan telescope. This work has been partly funded by the Australian Research Council (grants DP0342613 and DP0558836).

References

- Aguirre, A., Dow-Hygelund, C., Schaye, J., & Theuns, T. 2008, ApJ, in press (arXiv:0712.1239)
- Akerman, C. J., Carigi, L., Nissen, P. E., Pettini, M., & Asplund, M. 2004, A&A, 414, 931
- Allende Prieto, C., Asplund, M., & Fabiani Bendicho, P. 2004, A&A, 423, 1109
- Andersson, H., & Edvardsson, B. 1994, A&A, 290, 590
- Asplund, M., & García Pérez A. E. 2001, A&A, 372, 601
- Asplund, M., Grevesse, N., Sauval, A. J., Allende Prieto, C., & Kiselman, D. 2004, A&A, 417, 751
- Asplund, M. 2005, ARA&A, 43, 481
- Asplund, M., Grevesse, N., & Sauval, A. J. 2005, ASP Conference Series, 336, 25
- Asplund, M., Lambert, D. L., Nissen, P. E., Primas, F., & Smith, V. V. 2006, ApJ, 644, 229
- Barbuy, B. 1988, A&A, 191, 121
- Becker, G., D., Sargent W. L. W., Rauch, M., & Simcoe, R. A. 2006, ApJ, 640, 69
- Bensby, T., & Feltzing, S. 2006, MNRAS, 367, 1181
- Bernstein, R., Shtetman, S. A., Gunnels, S. M., Mochnacki, S., & Athey, A. E. 2003, SPIE, 4841, 1694
- Boesgaard, A. M., King, J. R., Deliyannis, C. P., Vogt, S. S. 1999, AJ, 117, 492
- Bromm, V., & Loeb, A. 2003, Nature, 425, 812
- Carigi, L., Peimbert, M., Esteban, C., & García-Rojas, J. 2005, ApJ, 623, 213
- Carollo, D., Beers, T. C., Lee, Y. S., et al. 2007, Nature, 450, 1020
- Chiappini, C., Romano, D., & Matteucci, F. 2003, MNRAS, 339, 63
- Chiappini, C., Hirschi, R., Meynet, G., et al. 2006, A&A, 449, L27
- Chieffi, A., & Limongi, M. 2002, ApJ, 577, 281
- Chieffi, A., & Limongi, M. 2004, ApJ, 608, 405
- Collet, R., Asplund, M., & Trampedach, R. 2007, A&A, 469, 687
- Dekker, H., D’Odorico, S., Kaufer, A., Delabre, B., & Kotzlowski, H. 2000, SPIE, 4008, 534
- Drawin, H. W. 1968, Zeitschrift f. Physik, 211, 404
- Drawin, H. W. 1969, Zeitschrift f. Physik, 225, 483
- El Eid, M. 2005, Nature, 433, 117
- Erni, P., Richter, P., Ledoux, C., & Petitjean, P. 2006, A&A, 451, 19
- Fabbian, D., Asplund, M., Carlsson M., & Kiselman, D. 2006, A&A, 458, 899
- Fabbian, D., Asplund, M., Barklem, P. S., & Kiselman, D. 2008a, A&A submitted
- Frebel, A., Johnson, J. L., & Bromm, V. 2007, MNRAS, 380, 40
- Gavilán, M., Buell, J. F. & Mollá, M. 2005, A&A, 432, 861
- Gustafsson, B., Karlsson, T., Olsson, E., Edvardsson, B., & Ryde, N. 1999, A&A, 342, 426
- Israelian, G., García López, R. J., & Rebolo, R. 1998, ApJ, 507, 805
- Kobayashi, C., Umeda, H., Nomoto, K., Tominaga, N., & Ohkubo, T. 2006, ApJ, 653, 1145
- Masana, E., Jordi, C. & Ribas, I. 2006, A&A, 450, 735
- Meléndez, J., Shchukina, N. G., Vasiljeva, I., & Ramírez, I. 2006, ApJ, 642, 1082
- Meynet, G., Ekström, S., Maeder, A., et al. 2008, AIP Conference Proceedings, 990, 212
- Nissen, P. E., Primas, F., Asplund, M., & Lambert, D. L. 2002, A&A, 390, 235
- Nissen, P. E., Akerman, C., Asplund, M., et al. 2007, A&A, 469, 319
- Ohkubo, T., Umeda, H., Maeda, K., et al. 2006, ApJ, 645, 1352
- Pettini, M., Zych, B. J., Steidel, C. C. & Chaffee, F. H. 2008, MNRAS, 385, 2011
- Ramírez, I., & Meléndez, J., 2005a, ApJ, 626, 446
- Ramírez, I., & Meléndez, J., 2005b, ApJ, 626, 465
- Reddy, B. E., Lambert, D. L., & Allende Prieto, C. 2006, MNRAS, 367, 1329
- Richard, O., Michaud G., & Richer, J. 2002, ApJ, 580, 1100
- Ryan-Weber, E. V., Pettini, M., & Madau, P. 2006, MNRAS, 371, L78
- Smiljanic, R., Pasquini, L., Primas, F., et al. 2008, MNRAS, 385, L93
- Spite, M., Cayrel, R., Plez, B., et al. 2005, A&A, 430, 655
- Wallerstein, G., Iben, I., Jr., Parker, P., et al., 1997, Reviews of Modern Physics, 69, 995
- Wolfe, A. M., Gawiser, E., & Prochaska, J. X. 2005, ARA&A, 43, 861
- Wiese, W. L., Fuhr, J. R., & Deters, T. M. 1996, J. Phys. Chem. Ref. Data Monograph, No. 7